Cell Mol Neurobiol (2009) 29:981–990
DOI 10.1007/s10571-009-9385-3

ORIGINAL PAPER

Immunohistochemical Study of Postnatal Neurogenesis After Whole-body Exposure to Electromagnetic Fields: Evaluation of Age- and Dose-Related Changes in Rats

Judita Orendáčová · Eniko Račeková · Martin Orendáč · Marcela Martončíková · Kamila Saganová · Kamila Lievajová · Henrieta Abdiová · Ján Labun · Ján Gálik

Received: 12 November 2008 / Accepted: 27 February 2009 / Published online: 21 March 2009

Abstract It is well established that strong electromagnetic fields (EMFs) can give rise to acute health effects, such as burns, which can be effectively prevented by respecting exposure guidelines and regulations. Current concerns are instead directed toward the possibility that long-term exposure to weak EMF might have detrimental health effects due to some biological mechanism, to date unknown. (1) The possible risk due to pulsed EMF at frequency 2.45 GHz and mean power density 2.8 mW/cm^2 on rat postnatal neurogenesis was studied in relation to the animal's age, duration of the exposure dose, and post-irradiation survival. (2) Proliferating cells marker, BrdU, was used to map age- and dose-related immunohistochemical changes within the rostral migratory stream (RMS) after whole-body exposure of newborn (P7) and senescent (24 months) rats. (3) Two dose-related exposure patterns were performed to clarify the cumulative effect of EMF: short-term exposure dose, 2 days irradiation (4 h/day), versus long-term exposure dose, 3 days irradiation (8 h/day), both followed by acute (24 h) and chronic (1–4 weeks) post-irradiation survival. (4) We found that the EMF induces significant age- and dose-dependent changes in proliferating cell numbers within the RMS. Our results indicate that the concerns about the possible risk of EMF generated in connection with production, transmission, distribution, and the use of electrical equipment and communication sets are justified at least with regard to early postnatal neurogenesis.

Keywords Cumulative effect · Non-ionizing radiation · Rostral migratory stream · Quantitative analysis · BrdU immunohistochemistry · Newborn · Senescent

J. Orendáčová (✉) · E. Račeková · M. Martončíková · K. Saganová · K. Lievajová · J. Gálik
Institute of Neurobiology, Center of Excellence, Slovak Academy of Sciences, Šoltésovej 4, Košice 040 01, Slovak Republic
e-mail: orendac@saske.sk

M. Orendáč
Faculty of Electrical Engineering and Informatics, Department of Theoretical Electrotechnics and Electrical Measurement, Technical University of Košice, Letná 9, Košice 042 00, Slovak Republic

J. Labun
Faculty of Aeronautics, Department of Avionics, Technical University of Košice, Rampová 7, Košice 040 01, Slovak Republic

H. Abdiová
Stredná zdravotnícka škola, Moyzesova 17, Košice 040 01, Slovak Republic

Introduction

Electromagnetic Fields

The electromagnetic spectrum encompasses a wide variety of electromagnetic fields (EMFs) including static fields, radio-frequency fields, UV radiation, visible light, and X-ray radiation. EMFs are characterized by their frequency or wavelength; wavelength is inversely proportional to frequency. At the lower end of the electromagnetic spectrum, it is customary to refer to the frequency, while at the upper end, wavelength is usually used (Ahlbom and Feychting 2003). Electromagnetic waves at high frequencies, physically belonging to "non-ionizing" radiation, are called electromagnetic radiation (EMR) or radio-frequency radiation. Radio-frequency fields, in the frequency range from 1 MHz to 300 GHz, are only a part of the EMF spectrum,

and their main sources are, for example, radio, television, radar, cellular telephone antennas, and microwave ovens. The absorbed radio-frequency energy in tissue is quantified using the specific absorption rate—SAR (W/kg), which is the primary parameter used when discussing the health risk due to EMF power absorption in the body, or using the maximum permissible exposure value, which is the upper limit of EMR power density (mW/cm^2) exposure for biological tissues (Martens et al. 1995). In our experiment we used the power density unit as the exposure value parameter.

Neurogenesis

It is evident that at least two regions of the adult brain are responsible for proliferation and migration of neural cell precursors: the subventricular zone (SVZ) and hippocampal dentate gyrus (Cayre et al. 2002; Doetsch 2003). The SVZ, which lines most of the lateral wall of the lateral ventricles, persists as a germinal zone into adulthood and thus functions as the largest region of neurogenesis in the adult brain (Doetsch and Alvarez-Buylla 1996). Cells born in the SVZ migrate via a restricted pathway, called the rostral migratory stream (RMS), to the olfactory bulb (OB) where they differentiate into local interneurons (Altman 1969; Lois and Alvarez-Buylla 1994). The proliferating cells marker, bromodeoxiuridine (BrdU) is regularly used to label proliferating cells (in the S-phase) within the SVZ–OB pathway. BrdU immunohistochemistry has regularly been used for estimating proliferating cell numbers in the RMS of rats to map physiological dynamics at various postnatal ages (Martončíková et al. 2006) and in some experimental interventions such as in experimental ablation of OB (Kirschenbaum and Goldman 1995; Kirschenbaum et al. 1999; Račeková et al. 2002), after stress induced by maternal separation (Lievajová et al. 2008; Račeková et al. 2008), or after environmental enrichment conditions (Martončíková et al. 2008). To express the dynamics of proliferation, these immunohistochemical studies utilize quantitative analyses.

Irradiation and Neurogenesis

Studies of the possible risk of EMF for nervous tissue have regularly been published since the mid-twentieth century (Baranski and Edlwejn 1967, 1968; Goldberg 1996). The current discussion is centered on whether long-term low-level exposure to EMF can evoke neuropathological responses and influence people's well-being. Despite numbers of neurobiological studies demonstrating that various EMF frequencies induce changes in the nervous tissue of experimental animals, evidence for EMF impact on the health of the nervous system remains uncertain. Our review article focusing on morphological findings in experimental animals subjected to EMF (Orendáčová et al. 2007) shows that the rat is the most often used animal in such experiments, and that the blood–brain barrier is one of the first and the most studied morpho-functional units of nervous tissue in this field (Oscar and Hawkins 1977; Salford et al. 1992, 1993, 1994). Salford et al. (2003) focused on the possibility that microwave exposures causing blood–brain barrier damage could cause damage to the brain itself. In their study, highly significant evidence for neuronal damage in the cortex, hippocampus, and basal ganglia was found. Possibly due to the fact that the brain has long been regarded as a radio-resistant organ, composed of non-dividing cells, experimental observations of post-irradiation changes in neurogenesis appeared only at the end of the last century (Tada et al. 1999, 2000). Recently, Bálentová et al. (2006) showed that a non-lethal dose of 3 Gy ionizing radiation significantly changes the BrdU$^+$ cell number within the RMS of adult rats. The authors demonstrated the dynamics of post-irradiation changes (Bálentová et al. 2007a) and even transgenerational effects of ionizing radiation. Paternal exposure, 25 days before conception, influences BrdU$^+$ cell numbers in the offspring during the first postnatal month (Bálentová et al. 2007b).

In this study, we used BrdU immunohistochemistry to map age-related changes in proliferation activities within the RMS after whole-body EMF exposure of the newborn and senescent rats. The results of two different EMF dose-related patterns, short- and long-term exposure, were quantitatively evaluated after acute and chronic post-irradiation survivals.

Methods

The experimental procedure was performed with approval from the Animal Care Committee of the Institute of Neurobiology, Slovak Academy of Sciences. Wistar albino rats were used in this experiment.

Experimental Intervention

The rats were exposed to a pulse-wave EMF of 2.45 GHz, at mean power density 2.8 mW/cm^2, in a purpose-designed exposure chamber. The chamber-exposure complex was designed to enable the freely moving rats remain in their own breeding cage during irradiation emitted from the EMR source (a microwave oven) and to prevent radiation spreading into the surroundings (Orendáč et al. 2005a, b). The homogeneity of the emitted EMF was mapped inside the chamber and inside the animal cage by a spectral analyzer at various EMF modes of the microwave emitter.

In this way, the most suitable place for the animal breeding cage placement, i.e., the place where the emitted microwave fields are as homogeneous as possible, was identified. The EMF doses were applied to animals, which had ad libitum access to food and water during their stay in the special housing conditions.

General Remarks on the Experimental Animal Groups

We drew up a synoptical complete setting of the experimental groups (Table 1) to make orientation easier in the applied EMF duration and doses, the irradiated animals' ages, the timing of post-irradiation survival, and the observed results.

Short- and Long-Term Irradiation Dose Experimental Groups

Two experimental groups were created in which two different exposure doses were related to the exposure durations. The animals irradiated for 2 days (4 h/day) were considered as the short-term exposure dose group, while animals in the long-term exposure group were irradiated for 3 days (8 h/day).

Newborn and Senescent Experimental Groups

The animals in the newborn group were irradiated with short- and long-term exposures on the 7th postnatal day (P7). The animals in the senescent group were irradiated with short- and long-term exposure doses at 24 months of age.

Acute and Chronic Post-Irradiation Survival

In the newborn short-term exposure group, acute post-irradiation changes (API) were mapped after 1 day of post-irradiation survival, and chronic post-irradiation changes (CPI) were mapped after 1, 2, 3, and 4 weeks survival. In the newborn long-term exposure rats, CPI observations were stopped after 3 weeks' survival due to the severe retardation of the animals' bodyweight and growth. In the newborn experimental animals irradiated at P7, it should be noted that with respect to the 2 and/or 3 days of irradiation duration, the mapping of API changes (1 day after irradiation) was performed in animals biologically at P10 or P11 age, and for this reason, only the control rats at P10 were used. Mapping of CPI changes after 1 week of post-irradiation survival were carried out on P14 rats, etc.

In the senescent short- and long-term exposure dose group, the API changes were mapped after 1 day of post-irradiation survival, and the CPI observations were stopped after 3 weeks of survival due to the insignificant changes in proliferation observed at this duration of post-irradiation survival.

Control Groups

The $BrdU^+$ cell densities within the RMS of newborn rats at P10, P14, P21, P28, and P35 were used as controls to which the newborn experimental group rats of the same ages were related. The senescent controls were used at 24 months of age.

Tissue Sampling and Immunohistochemical Treatment

To label proliferating cells at the end of post-irradiation survival, the animals were first lightly anesthetized by Halotane inhalation, then received a single i.p. injection of cell proliferation marker BrdU (50 mg/kg of the body weight, Sigma). Two hours after BrdU administration, the rats were deeply anesthetized with a mixture of xylazine and ketamine and intracardially (at 15 kPa) perfused with

Table 1 Compendium of all experimental groups displaying the EMF doses and durations, the irradiated animals' ages, the post-irradiation survival timings, the results, and notes

EMF exposure doses and duration	Age of rats at irradiation	Post-irradiation survival		Post-irradiation changes in proliferation	Notes on the CPI survival choice
		API	CPI		
Short-term 2 days irradiation (4 h/day)	Newborn P7	1 day	1, 2, 3, 4 weeks	Significant diphasic increase/decrease of $BrdU^+$ cells	Continuous dynamic of changes after API and CPI
Long-term 3 days irradiation (8 h/day)	Newborn P7	1 day	1, 2, 3 weeks	Immediate and permanent decrease of $BrdU^+$ cells	Stagnation of rats' development and bad physical state
Short-term 2 days irradiation (4 h/day)	Senescent 24 months	1 day	1, 2, 3 weeks	Negligible changes to the senescent control values	No dynamic of changes; no reason to persist with survival
Long-term 3 days irradiation (8 h/day)	Senescent 24 months	1 day	1, 2, 3 weeks	Negligible changes to the senescent control values	No dynamic of changes; no reason to persist with survival

4% paraformaldehyde in 0.1 M phosphate buffer at pH 7.4 for 5 min in neonates and 10 min in the older animals. After perfusion, the brains were immediately removed from the skulls, postfixed in the same fixative solution for 4 h, and cryoprotected by immersion in PB containing 30% sucrose overnight. Sagittal serial sections (42 μm) were cut on a cryostat and processed for routine BrdU immunohistochemistry (Martončíková et al. 2006).

Quantitative Analysis

All the sections were examined using an Olympus-BX51 light microscope under oil immersion lens at 40× magnification. Serial digital images were obtained using a DP50 camera connected with DP Image Tool (version 3.0). We evaluated only those sections where the whole extent of the RMS was visible (4–6 sections/RMS). Images were captured for evaluation of these sections. The number of $BrdU^+$ cells was counted in three specific parts of the RMS—in the vertical arm, horizontal arm and in the elbow—using Dissector software version 2.0 (Tomori et al. 2001), which allows application of the point-counting method needed for unbiased estimation of the particle volume density in a three-dimensional space (Bálentová et al. 2007a). The outcomes were expressed as proliferating cell density, i.e., the number of the $BrdU^+$ cells/mm^3. The values of the experimental and control groups were evaluated with one-way ANOVA and Tukey-Kramer tests, and the results are presented as mean values ± S.E.M. Statistical significance was assumed for $P < 0.05$ and $P < 0.01$.

Results

In sagittal sections, the RMS was easily recognized as a morphologically distinct pathway, spanning the anterior tip of the lateral ventricle and the OB. Within the RMS in caudo-rostral direction, three parts topographically follow one after another: the vertical arm, elbow, and horizontal arm. The RMS thickness and shape are characteristic for each period of rat age. In newborn rats, the RMS diameter is relatively greater than in senescent rats. The RMS shape in newborn rats between P7 and P14 looks like a "U"-shaped column, and from P14 till the senescent age, it is visible as a typical "L"-shaped column.

Immunohistochemical Findings in Newborn Rats

Short-Term Irradiation

In this experimental group, 2 days (4 h/day) of whole-body EMF exposure was applied to newborn rats at P7 age. Two different post-irradiation periods, API after 1 day survival and CPI after 1–4 weeks survival, were studied using BrdU immunohistochemistry. The proliferating cells density was evaluated in the vertical arm, elbow, and horizontal arm separately.

After API survival, short-term exposure induced the most significant changes in $BrdU^+$ cell numbers in all the evaluated experimental groups. There was a very large number of $BrdU^+$ cells scattered within each part of the RMS (Fig. 1). Numerous round dark-brown cells were regularly dropped also within the SVZ, the neurogenetic region intimately connected with the lateral ventricle. In contrast to these findings, however, in the control rats, the number of $BrdU^+$ cells within the RMS was diminished when matching them to the API rats of the same age. Graphical demonstration of the API changes and controls (Fig. 2) showed significant changes in the vertical arm, elbow, and horizontal arm. A synoptical view of control versus API proliferation in the RMS at P10 age demonstrates that $BrdU^+$ cell density reached its minimum values

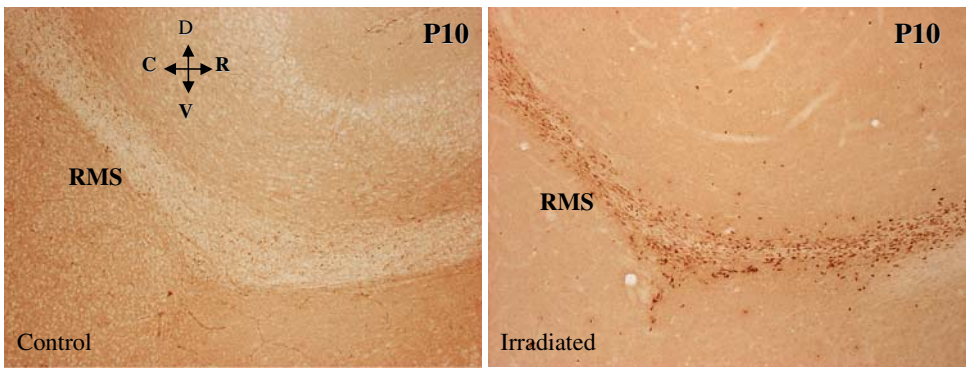

Fig. 1 Newborn rats irradiated at P7 by short-term (2 days-4 h/day) EMF and submitted to API survival. Representative micrographs of the BrdU immunohistochemistry at P10 age demonstrate significant differences of proliferation activity in the control (*left*) and irradiated (*right*) rats. Abundant $BrdU^+$ cells within the RMS detected immediately after EMF exposure represent the most significant increase of post-irradiation proliferation activity observed in all the experimental groups of our study

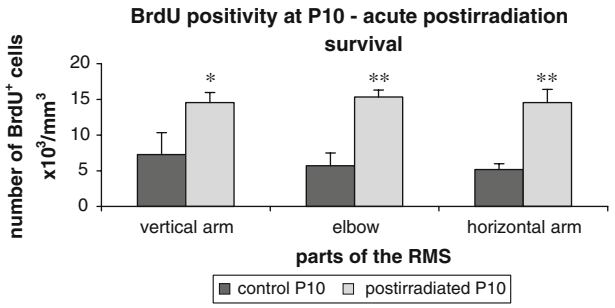

Fig. 2 Newborn rats irradiated at P7 by short-term (2 days-4 h/day) EMF and submitted to API survival. Quantification of the $BrdU^+$ cells in the vertical arm, elbow, and horizontal arm shows significant API changes in comparison to the same RMS parts in the control rats of the same ages. * Significant differences $P < 0.05$; ** Highly significant differences $P < 0.01$

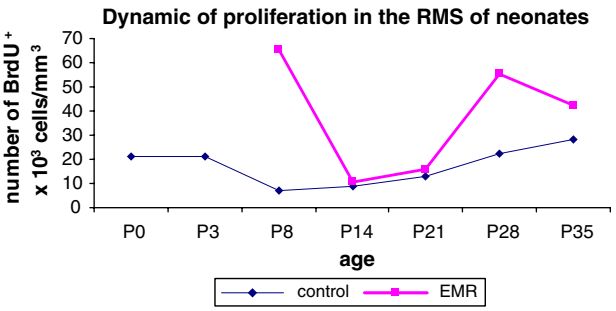

Fig. 3 Newborn rats irradiated at P7 by short-term (2 days-4 h/day) EMF and submitted to API/CPI survivals. Graphical demonstration of the $BrdU^+$ cells during post-irradiation survival (solid line) discloses double peaks' dynamics of proliferation activity: at API and CPI survival (P28 rats). The most significant post-irradiation increase of the $BrdU^+$ cells coincides with the physiological decrease of $BrdU^+$ cells in the P8 controls (dashed line). Each datum point represents a mean of three rats

in the control rats and its maximum values after the short-term exposure dose and API survival (Fig. 3). The CPI changes were assessed 1, 2, 3, and 4 weeks after short-term EMF exposure applied to P7 rats. Estimation of $BrdU^+$ cell density at each post-irradiation week disclosed the dynamics of post-irradiation changes in cell proliferation. This was the only CPI experimental group displaying dynamics of post-irradiation changes. During the first week of CPI survival, i.e., in P14 rats, the maximum values of $BrdU^+$ cells, reached after API survival, started to rapidly decrease. After 2 weeks of post-irradiation survival, the number of $BrdU^+$ cells reached the minimum of all the values, which occurred during the post-irradiation survival. During the next 2 weeks of post-irradiation survival, the number of $BrdU^+$ cells increased till the second peak of the proliferating cell values, and then at the end of the 4th week of CPI survival, the number of $BrdU^+$ cells declined toward the values characteristic for the control rats of young adult age. Graphical demonstration of the API and CPI changes in their consequences and comparison to the controls disclosed diphasic significant increase in the proliferating cell densities within the RMS of the rats irradiated at P7 age (Fig. 3). In these rats the first peak appears in the API period and inversely coincides with the steepest fall in the $BrdU^+$ cell density recorded in the control rats of the same age. The second peak of $BrdU^+$ cell density appeared after 3 weeks of CPI survival, and then the proliferating cell number decreased toward the control values of young adult rats at P35 age. In the control rats, the number of $BrdU^+$ cells within the RMS increased little by little from P10 till the end of the first postnatal month.

Similarly, graphical demonstration of the API and CPI proliferation activities in the separate RMS parts revealed significant differences within each part of the RMS during the first 3 post-irradiation weeks (Fig. 4) in relation to the control rats at P10 age. The numerical values of the $BrdU^+$ cells expressed separately in the vertical arm, elbow, and horizontal arm generally copied the double-peak pattern of increase in proliferating cell numbers within the whole RMS.

Long-Term Irradiation

The animals of this experimental group were exposed to EMF for 8 h/day for 3 days at P7 age. In these animals, distinct macroscopical observations preceded the BrdU immunohistochemical findings. Significant growth retardation was evident in the irradiated rats from the first week of CPI survival. The average bodyweight of the hypotrophic rats at P28 age, i.e., 3 weeks after irradiation, was reduced by 50% in comparison with the short-term irradiated rats or control rats of the same age. At the microscopical level, only a few BrdU-labeled cells were visible within the RMS as a characteristic outcome of diminished proliferation activity after the long-term exposure of the newborn rats. This rapidly diminishing proliferation activity appeared immediately after API survival and persisted without variation as a significant change till the 3rd week of CPI survival (Fig. 5). Because there was no post-irradiation survival dynamic in this experimental group and because of the very bad physical state of the animals, the post-irradiation survival was stopped after 3 weeks of duration.

Immunohistochemical Findings in Senescent Rats

Short- and Long-Term Irradiation

There was no difference in the results between the short- and long-term irradiation, i.e., between the dose-related groups of senescent age. Neither the short-term nor the

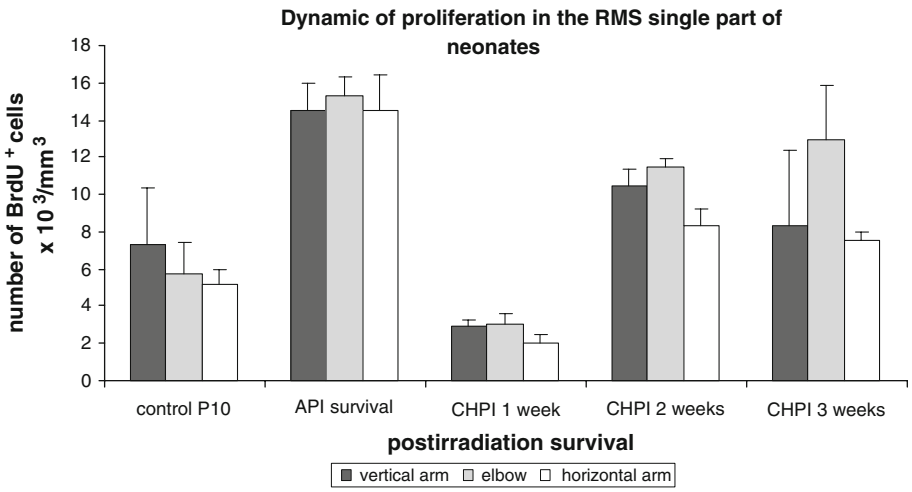

Fig. 4 Newborn rats irradiated at P7 by short-term (2 days-4 h/day) EMF and submitted to API/CPI survivals. Quantifications of the BrdU$^+$ cells in the vertical arm, elbow, and horizontal arm of the RMS in the API survival and the first 3 weeks of the CPI; comparison with the respective RMS parts of the control at P10 is demonstrated. The most significant changes appeared immediately post-irradiation, i.e., in the API survival and after 1 week of the CPI survival

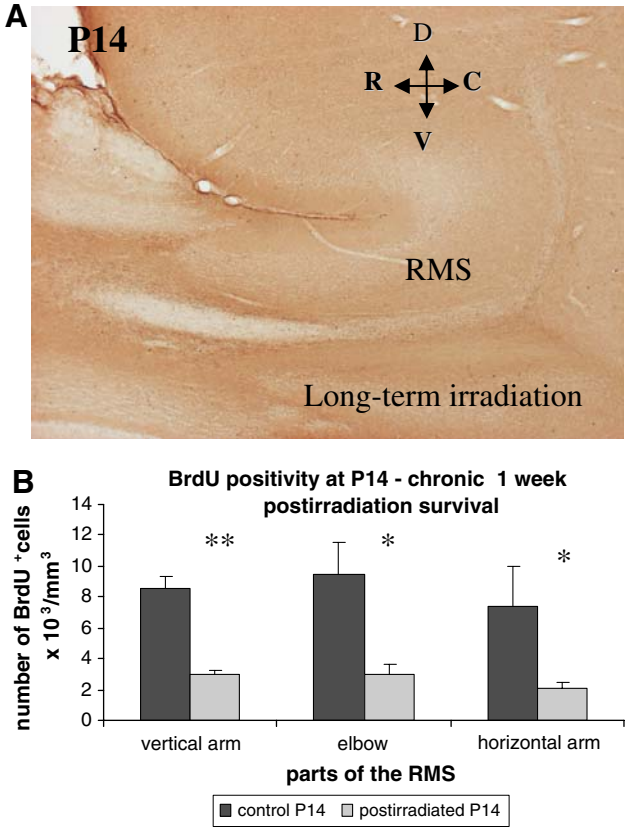

Fig. 5 Newborn rats irradiated at P7 by long-term (3 days-8 h/day) EMF and submitted to API/CPI survival. Representative micrographs of the BrdU$^+$ cells diminishing within the RMS (**a**). Graphical demonstration of the BrdU$^+$ cells decreasing (**b**) in the vertical arm, elbow, and horizontal arm at P14 age, i.e., 1 week post-irradiation and the respective control. * Significant differences $P < 0.05$; ** Highly significant differences $P < 0.01$

long-term EMF exposure of the 24-month-old rats induced any significant changes in BrdU$^+$ cell numbers within the RMS in comparison to those in the the senescent controls (Fig. 6). In accordance with these findings, quantitative analyses of each part of the RMS, vertical arm, elbow, and horizontal arm, disclosed insignificant changes in BrdU$^+$ cell numbers after both short-term and long-term exposure doses. Negligible deviations in BrdU$^+$ cell numbers during CPI survival, even after long-term exposure of the senescent rats in comparison to the senescent controls, are shown in Fig. 7. There was no dynamic of proliferation changes during the 3 weeks of CPI survival, and for this reason, we did not continue with observations after that post-irradiation time in the senescent experimental group.

Discussion

The data presented here reveal the possible risk of pulsed EMF for rat postnatal neurogenesis in relation to the animal age, and similarly to the applied EMF doses. Two extremes of evaluated ages, newborn and senescent, were meant to represent a pivotal distinction between the risks of EMF for neurogenesis. Two different irradiation doses, short-term, 2 days exposure (4 h/day), versus long-term, 3 days exposure (8 h/day), were supposed to clarify the possible cumulative effect of EMF. The dynamics of changes were observed from the acute, 24-h post-irradiation survival, till the chronic, 1–4 weeks of post-irradiation survival. Our data show: (1) significant increase in BrdU$^+$ cell numbers and the dynamics of post-irradiation changes within the RMS when the EMF whole-body exposure is applied to newborn rats of P7 age; (2) permanent decrease in BrdU$^+$ cell numbers within the RMS after long-term irradiation when the EMF whole-body exposure is applied to newborn rats of P7 age; (3) negligible changes in proliferation activity when the EMF whole-body exposure is applied to senescent rats. It is evident that EMF exposure induces dose-dependent changes in proliferation within the RMS in newborn rats. We suppose that this age-dependent post-irradiation predetermination of proliferation activity could

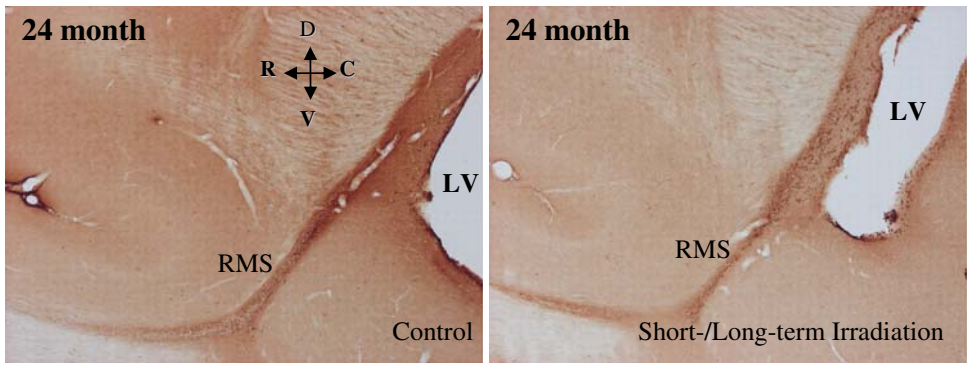

Fig. 6 Senescent rats irradiated by long-term (3 days-8 h/day) EMF and submitted to CPI survival. Representative micrographs show equal $BrdU^+$ cells densities in the senescent control rats (*right*) and the CPI rats after 3 weeks survival (*left*)

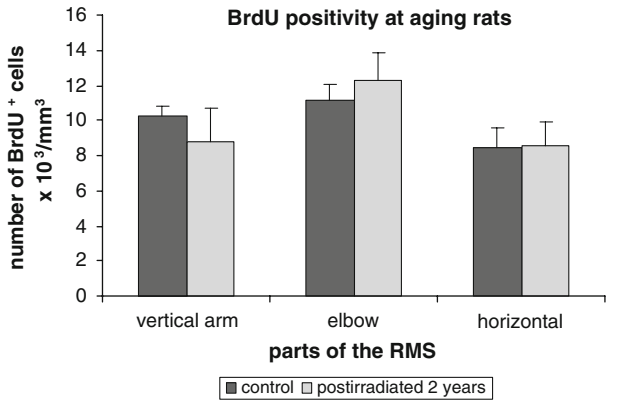

Fig. 7 Senescent rats irradiated by long-term (3 days-8 h/day) EMF and submitted to CPI survival. Quantification of the $BrdU^+$ cells within each part of the RMS after the CPI survival and in the respective senescent control show no significant differences of proliferation after 3 weeks of post-irradiation survival

be closely connected with the processes of postnatal maturation and aging under physiological conditions.

The availability of BrdU immunostaining in our experimental paradigm has been improved by several experiments. Single i.p. injection of 50 mg/kg of BrdU, used by us, has been shown to be the dose that labels every cell in the S-phase region of the pseudostratified ventricular eithelium and has no apparent toxic effects (Zigova et al. 2002). Regarding the survival time following BrdU administration, we have chosen the possible shortest interval (i.e., 2 h) of the marker incorporation, which allows detection of dividing cells. Dayer et al. (2003) while comparing the number of BrdU-labeled cells in the dentate gyrus of adult rats at several time points after labeling showed that after the initial increase between 2 and 24 h, the number of BrdU-labeled cells did not change significantly. In our previous study, we have also shown that the 2-h survival after BrdU administration labels proliferating cells in the RMS of rats (Martončíková et al. 2006). Moreover, the 2-h survival is the most proper period for immunohistochemical detection of early gene c-fos, immediately expressed after many kinds of injuries. Thus, 2-h period of the BrdU incorporation offers possibility to continue our experimental paradigm by c-fos immunohistochemistry for observations of the very API changes and to make direct comparison of recently published data with the results obtained in the future. Our preliminary recent data (Orendáčová et al. 2008) show that the c-fos expression in the SVZ, not in the RMS, increases significantly, and similarly in the newborn and senescent rats even after a single 2-h irradiation by EMF of mean power density 2.8 mW/cm^2.

Age-Dependency of Neurogenesis Dynamics in Physiological Conditions

Previously the authors have reported that the postnatal cell proliferation within the RMS of newborn rats is a very dynamic process characterized by the presence of a very large number of proliferating cells between P1 and P7, significant decrease in $BrdU^+$ cell numbers between P7 and P10, and afterward a continuous increase in $BrdU^+$ cells till P28, which is the level of young adult rats (Martončíková et al. 2006). We have shown that the physiological fall in proliferating cell numbers in P7–P10 rats coincides with the appearance of the first NADPHd-positive cells (Račeková et al. 2003, 2005). Starting from P14 age, NADPHd-positive cells constantly reside in each part of the RMS, and from that period, proliferation continues in the presence of nitric oxide (NO). We have found that despite the known anti-proliferating effect of NO, cell proliferation even increases significantly till P28 postnatal age. Our results also demonstrate the continuous increase in NO-positive cells in the RMS of adult 5-month-old rats, highly significant in comparison to the P14 newborn rats, and a further significant increase in senescent, 20-month-old rats. These results indicate that NO actually plays a negative role in neurogenesis control. Some other observations have found evidence of age-related decline in $BrdU^+$ cell numbers in the dentate gyrus, but not in the lateral ventricle wall, of ≥2-year-old animals (Kuhn et al. 1996; Lichtenwalner et al. 2001). Multiple studies have shown in adult rats, mice, and tree shrews, that the rates of

neurogenesis begin to slow down before 1 year of age, i.e., well before the onset of senescence (Kuhn et al. 1996; Leuner et al. 2007).

Age- and Dose-Dependency of Post-Irradiation Neurogenesis Dynamics

Our previous observations of the physiological slowing down of proliferation activities in P7 newborn rats and at senescent age determined our choice of these two extreme ages, both displaying slowdown (transitional in newborns and permanent in senescent animals) proliferation activities, in the age-related study. We expected that the brain neurogenetic region should be vulnerable to non-ionizing radiation, as high proliferation activity is characteristic for that age. Thus, the aging brain should be more radioresistant due to its slower proliferating activity as well as the brain in newborns at P7–P10 age. Our results presented here as the EMF impacts on cell proliferation within the RMS are in accordance with our expectations, but only in the senescent rats. The high radio sensitivity of the newborns, regardless of the fact that EMF application coincided with the transitional period of physiological decrease in proliferation activity at P7–P10, and the radio resistance of the senescent rats, also exposed at a time of physiological decrease in proliferation activity, indicate, not surprisingly, the age dependence of the neurogenesis. But one unexpected finding was that proliferation activity in the senescent rats ran as a distinctly paced process, not disturbed by the long-term (high dose) EMR either in acute or chronic post-irradiation survival.

Recently, it has become well known that ionizing radiation, as one of the strongest cytotoxic factors, induces significant injury in the adult brain. It has been used for depleting the stem cells of the subependyma to study what role the neural stem cells play in brain injury (Tada et al. 1999). The BrdU immuno-morphometric approach has shown clear radiation-dose dependencies in the long-term impairment of subependymal repopulation following damage by ionizing irradiation in adult rats. There was progressively more stem cell damage with increasing radiation dose, between 2 Gy and 15 Gy, up to 180 days after treatment. Although these results refer to changes within the subependyma after ionizing radiation and our observations concerning, namely, the migratory stream with respect to non-ionizing radiation, we found similarity between both sets of findings. Our dose-dependent observations showed evidence that also non-ionizing radiation at high doses, or long-term EMF irradiation, induces long-lasting impairment of proliferation within the olfactory neurogenetic region when applied to newborn rats. The cumulative effect of EMFs manifested itself also macroscopically as severe malnutrition of the animals after long-term irradiation, inducing olfactory dysfunction due to the depletion of stem cells and proliferation activity within the RMS visible at microscopical level as diminishing of the $BrdU^+$ cell density. Only the newborn rats were significantly radio sensitive in our dose-related observations. This means that the cumulative effect of EMF functions as a strong cytotoxic factor inducing significant olfactory dysfunction by disqualification of proliferation within the RMS of newborn rats.

Multiple studies have shown that neurogenesis increases in the SVZ after brain injury, and it is coupled with migration of young neurons from the SVZ toward the non-olfactory bulb regions, but this migration is not at the expense of the RMS (Sundholm-Peters et al. 2005). In accordance with these results, Bálentová et al. (2006, 2007a, b) interpret their findings of proliferating cell numbers significantly increasing in the whole RMS during the two post-irradiation weeks after 3 Gy irradiation applied to adult rats, rather as induced slowing down of the proliferating cells' migration than as increasing of the cell division. Although these authors did not evaluate the early newborn post-irradiation periods, it seems that the adult age post-irradiation increase in proliferation is in good accordance with our observations of the newborn post-irradiation dynamics observed during the first two post-irradiation weeks. The post-irradiation increase in $BrdU^+$ cell numbers is considered to be a consequence of radiation-induced damage to DNA and resulting inhibition of cell-cycle progress (Dasika et al. 1999; Melo and Toczyski 2002).

We assume that the characteristic diphasic increase in $BrdU^+$ cells within the RMS induced by short-term EMF exposure, and the permanent diminishing of $BrdU^+$ cells within the RMS after long-term EMF exposure, both applied at P7 rats, show the boundary between non-genotoxic and genotoxic doses of irradiation. Irradiation, as a genotoxic agent, activates the cell-cycle checkpoint and results in temporary cell growth arrest, which allows DNA repair before proliferation or induces cell apoptosis (Erenpreisa and Cragg 2001; Uberti et al. 2001; Wang et al. 2004). Our data suggest that due to the cumulative effect of 3 days (8 h/day) of irradiation, surviving stem cells are unable to regenerate and migrate even after 3 weeks post-irradiation so we consider the dose as genotoxic.

Conclusions

We found that whole-body exposure to pulsed EMF of mean power density 2.8 mW/cm^2 induces significant age- and dose-related changes in proliferation within the RMS in rats. The most significant age-related changes, with their characteristic double-peaked post-irradiation dynamics, were observed only in the rats irradiated at P7 age with the

short-term 2 days (4 h/day) exposure dose. Similarly, the most significant dose-related changes, immediate and permanent diminishing of proliferation, were observed only in the rats irradiated at P7 age with the long-term 3 days (8 h/day) exposure dose. In the senescent rats, there were no significant changes within the RMS. Our findings indicate that although proliferation within the RMS runs during the whole of postnatal life, there are age-related characteristics in this neurogenetic region.

Acknowledgments This work was supported by the VEGA Grants: 2/0058/08; 2/0092/08; 2/0147/09 and the APVV Grants: 51-0021-05; 51-0314-06.

References

Ahlbom A, Feychting M (2003) Electromagnetic radiation. Br Med Bull 68:157–165. doi:10.1093/bmb/ldg030

Altman J (1969) Autoradiographic and histological studies of postnatal neurogenesis. IV. Cell proliferation and migration in the anterior forebrain, with special reference to persisting neurogenesis in the olfactory bulb. J Comp Neurol 137:433–458. doi:10.1002/cne.901370404

Bálentová S, Račeková E, Mišúrová E (2006) Cell proliferation in the adult rat rostral migratory stream following exposure to gamma irradiation. Cell Mol Neurobiol 26:1131–1139. doi:10.1007/s10571-006-9067-3

Bálentová S, Račeková E, Mišúrová E (2007a) Effect of low-dose irradiation on proliferation dynamics in the rostral migratory stream of adult rats. Folia Biol 53:74–78

Bálentová S, Račeková E, Mišúrová E (2007b) Effect of paternal exposure to gamma rays on juvenile rat forebrain. Neurotoxicol Teratol 29:521–526. doi:10.1016/j.ntt.2007.03.063

Baranski S, Edlwejn Z (1967) Electroencephalographic and morphological investigations on the influence of microwaves on the central nervous system. Acta Physiol Pol 18:517–532

Baranski S, Edlwejn Z (1968) Studies on the combined effect of microwaves and some drugs on bioelectric activity of the rabbit nervous system. Acta Physiol Pol 19:31–41

Cayre M, Malaterre J, Scotto-Lomassese S, Strambi C, Strambi A (2002) The common properties of neurogenesis in the adult brain: from invertebrates to vertebrates. Comp Biochem Physiol B Biochem Mol Biol 132(1):1–15. doi:10.1016/S1096-4959(01)00525-5

Dasika GK, Lin S-CJ, Zhao S, Sung P, Tomkinson A, Kee EY-H (1999) DNA damage-induced cell cycle checkpoints and DNA strand break repair in development and tumorigeneses. Oncogene 18:7883–7899. doi:10.1038/sj.onc.1203283

Dayer AG, Ford AA, Cleaver KM, Yassaee M, Cameron HA (2003) Short-term and long-term survival of new neurons in the rat dentate gyrus. J Comp Neurol 460:563–572

Doetsch F (2003) A niche for adult neural stem cells. Curr Opin Genet Dev 13(5):543–550. doi:10.1016/j.gde.2003.08.012

Doetsch F, Alvarez-Buylla A (1996) Network of tangential pathways for neuronal migration in adult mammalian brain. Proc Natl Acad Sci USA 93:14895–14900. doi:10.1073/pnas.93.25.14895

Erenpreisa J, Cragg MS (2001) Mitotic death: a mechanism of survival? A review. Cancer Cell Int 1:1–7. doi:10.1186/1475-2867-1-1

Goldberg RB (1996) Literature resources for understanding biological effects of electromagnetic fields. http://infoventures.com/emf/top/lit-rev.html. Accessed 28 Oct 2008. Part of EMF–Link http://infoventures.com Accessed 28 Oct 2008

Kirschenbaum B, Goldman SA (1995) Brain-derived neurotrophic factror promotes the survival of neurons arising from the adult-rat forebrain subependymal zone. Proc Natl Acad Sci USA 92:210–214. doi:10.1073/pnas.92.1.210

Kirschenbaum B, Doetsch F, Lois C, Alvarez-Buylla A (1999) Adult subventricular zone neuronal precursors continue to proliferate and migrate in the absence of the olfactory bulb. J Neurosci 19:2171–2180

Kuhn HG, DickinsonAnson H, Gage FH (1996) Neurogenesis in the dentate gyrus of the adult rats: age-related decrease of neuronal progenitor proliferation. J Neurosci 16:2027–2033

Leuner B, Kozorovitskiy Y, Gross CG, Gould E (2007) Diminished adult neurogenesis in the marmoset brain precedes old age. Proc Natl Acad Sci USA 104:17169–17173. doi:10.1073/pnas.0708228104

Lichtenwalner RJ, Forbes ME, Bennett SA, Lynch CD, Sonntag WE, Riddle DR (2001) Intracerebroventricular infusion of insulin-like growth factor-I ameliorates the age-related decline in hippocampal neurogenesis. Neuroscience 107:603–613. doi:10.1016/S0306-4522(01)00378-5

Lievajová K, Martončíková M, Orendáčová J, Račeková E (2008) Effect of maternal separation on proliferation activity in the rat forebrain. In: Abstracts of 6th international symposium on experimental and clinical neurobiology, September 2008, p 53

Lois C, Alvarez-Buylla A (1994) Long-distance neuronal migration in the adult mammalian brain. Science 264:1145–1148. doi:10.1126/science.8178174

Martens L, DeMoerloose J, DeWagter C, DeZutter D (1995) Calculation of the electromagnetic fields induced in the head of an operator of a cordless telephone. Radio Sci 30:415–420. doi:10.1029/94RS00508

Martončíková M, Račeková E, Orendáčová J (2006) The number of proliferating cells in the rostral migratory stream of rat during the first postnatal month. Cell Mol Neurobiol 26:1451–1459. doi:10.1007/s10571-006-9039-7

Martončíková M, Lievajová K, Orendáčová J, Račeková E (2008) The rostral migratory stream of neonatal and young rats after olfactory stimulation. In: Abstracts of 6th international symposium on experimental and clinical neurobiology, September 2008, p 57

Melo J, Toczyski D (2002) A unified view of the DNA-damage checkpoint. Curr Opin Cell Biol 14:237–245. doi:10.1016/S0955-0674(02)00312-5

Orendáč M, Feník A, Mojžiš M, Orendáčová J (2005a) Construction of radiofrequency fields whole body exposure system applicable in freely moving rats. In: Abstracts of 5th international symposium on experimental and clinical neurobiology, Folia Med Cassoviensia, p 82

Orendáč M, Feník A, Mojžiš M, Orendáčová J (2005b) Biological effects of electromagnetic radiation on living systems with respect to the brain. Psychiatrie suppl 2:83–85

Orendáčová J, Orendáč M, Račeková E, Maršala J (2007) Neurobiological effects of microwave exposure: a review focused on morphological findings in experimental animals. Arch Ital Biol 145:1–12

Orendáčová J, Račeková E, Orendáč M, Martončíková M, Saganová K, Abdiová H, Mojžiš M, Labun J (2008) Immunohistochemical study of postnatal neurogenesis in the whole-body electromagnetic fields exposed rats. In: Abstracts of 6th international symposium on experimental and clinical neurobiology, September 2008, p 68

Oscar KJ, Hawkins TD (1977) Microwave alteration of the blood-brain barrier system of rats. Brain Res 126:281–293. doi:10.1016/0006-8993(77)90726-0

Račeková E, Orendáčová J, Martončíková M, Žigová T, Sekerková G, Maršala J (2002) Developmental characteristics in adult forebrain

following neonatal unilateral olfactory bulbectomy. Neurosci Res Commun 31:1–9. doi:10.1002/nrc.10032

Račeková E, Orendáčová J, Martončíková M, Vanický I (2003) NADPH-diaphorase positivity in the rostral migratory stream of the developing rat. Dev Brain Res 146:131–134. doi:10.1016/j.devbrainres.2003.09.014

Račeková E, Martončíková M, Mitrušková B, Čížková D, Orendáčová J (2005) Age-related changes of NADPH-Diaphorase positivity in the rat rostral migratory stream. Cell Mol Neurobiol 25:1093–1105. doi:10.1007/s10571-005-8191-9

Račeková E, Danko J, Martončíková M, Lievajová K, Flešárová S, Orendáčová J (2008) Exogenous factors induced alteration of nitric oxide expression in the rat rostral migratory stream. In: Abstracts of 6th international symposium on experimental and clinical neurobiology, September 2008, p 75

Salford LG, Brun A, Eberhardt J, Malmgren L, Persson B (1992) Electromagnetic field-induced permeability of the blood–brain barrier shown by immunohistochemical methods. In: Norden B, Ramel C (eds) Interaction mechanism of low-level electromagnetic fields in living systems. Oxford University Press, Oxford, pp 251–258

Salford LG, Brun A, Eberhardt J, Persson B (1993) Permeability of the blood–brain barrier induced by 915 MHz electromagnetic radiation, continuous wave and modulated at 8, 16, 50, 200 Hz. Bioelectrochem Bioenerg 30:293–301. doi:10.1016/0302-4598(93)80088-C

Salford LG, Brun A, Sturesson K, Eberhardt J, Persson B (1994) Permeability of the blood–brain barrier induced by 915 MHz electromagnetic radiation, continuous wave and modulated at 8, 16, 50 and 200 Hz. Microsc Res Tech 27:535–542. doi:10.1002/jemt.1070270608

Salford LG, Brun A, Eberhardt J, Malmgren L, Persson B (2003) Nerve cell damage in mammalian brain after exposure to microwaves from GSM mobile phones. Environ Health Perspect 111:881–883

Sundholm-Peters NL, Yang HKC, Goings GE, Walker AS, Szele FG (2005) Subventricular zone neuroblasts emigrate toward cortical lesions. J Neuropathol Exp Neurol 64:1089–1100. doi:10.1097/01.jnen.0000190066.13312.8f

Tada E, Yang C, Gobbel GT, Lamborn KR, Fike R (1999) Long-term impairment of subependymal repopulation following damage by ionizing irradiation. Exp Neurol 160:66–77. doi:10.1006/exnr.1999.7172

Tada E, Parent JM, Lowenstein DH, Fike JR (2000) X-irradiation causes a prolonged reduction in cell proliferation in the dentate gyrus of adult rats. Neuroscience 99:33–41. doi:10.1016/S0306-4522(00)00151-2

Tomori Z, Krekule I, Kubínová L (2001) Disector program for unbiased estimation of particle number, numerical density and mean volume. Image Anal Stereol 20:119–130

Uberti D, Piccioni L, Cadei M, Grigolato P, Rotter V, Memo M (2001) P53 is dispensable for apoptosis but controls neurogenesis fo mouse dentate gyrus cells following gamma-irradiation. Brain Res Mol Brain Res 93:81–89. doi:10.1016/S0169-328X(01)00180-2

Wang B, Ohyama H, Shang Y, Tanaka K, Aizawa S, Yukawa O, Hayata I (2004) Adaptive response in embryogenesis: existence of two efficient dose-rate ranges for 0.3 Gy of priming irradiation to adapt mouse fetuses. Radiat Res 161:264–272. doi:10.1667/RR3141

Zigova T, Sanberg PR, Sanchez-Ramos J (2002) Neural stem cells: methods and protocols. In: Humana Press Inc. (ed) Analysis of cell generation in the telencephalic neuroepithelium, New Jersey, pp 101–113